Signatures of the 3-day wave in the low-latitude and midlatitude ionosphere during the January 2010 URSI World Day campaign

Guiping Liu,[1] Scott L. England,[1] Thomas J. Immel,[1] Karanam K. Kumar,[2] Geetha Ramkumar,[2] and Larisa P. Goncharenko[3]

Received 1 February 2012; revised 26 March 2012; accepted 9 April 2012; published 6 June 2012.

[1] Recent studies of the equatorial ionosphere have found evidence of forcing by atmospheric Ultra Fast Kelvin (UFK) waves. This study investigates the quasi-3-day UFK wave and its effects on the variations of the ionosphere at low latitudes and midlatitudes using coordinated observations of both the atmosphere and ionosphere during the January 2010 URSI World Day campaign. The global maps of TEC from the IGS ground-based GPS product demonstrate a 3-day periodic variation during January 15–25. This variation has the largest amplitude at 15° magnetic latitude and extends into lower latitudes. Simultaneously, a 3-day wave is observed in the mesosphere in the zonal wind measurements by a meteor radar at the magnetic equator. The latitudinal range of the TEC variation (20°S–20°N) is also consistent with that of the 3-day wave. The Incoherent Scatter Radar (ISR) observations show a 3-day signature in vertical ion drifts over Jicamarca (11.9°S, 76°W) and in the electron densities in the top side of ionosphere measured from Millstone Hill (42.6°N, 71.5°W). This signature is consistent with the fountain effect in the equatorial region, and shows the impact on the topside ionosphere at midlatitudes. The UFK wave is trapped within ±30° geographic latitude, but this study shows that the effects of the wave could reach the ionosphere at the higher latitude even as high as 40°N (50°N magnetic latitude).

Citation: Liu, G., S. L. England, T. J. Immel, K. K. Kumar, G. Ramkumar, and L. P. Goncharenko (2012), Signatures of the 3-day wave in the low-latitude and midlatitude ionosphere during the January 2010 URSI World Day campaign, *J. Geophys. Res.*, *117*, A06305, doi:10.1029/2012JA017588.

1. Introduction

[2] The most dense plasma in the F-region ionosphere (at 200–600 km altitude) often exists in a two-banded structure at 15°–20° latitude away from the magnetic equator [*Namba and Maeda*, 1939; *Appleton*, 1946]. This two-banded structure is referred to as the equatorial ionospheric anomaly (EIA). The EIA is produced by the process called the fountain effect, in which the plasma is moved upward and poleward by the dynamo electric fields driven by neutral winds in the E-region (at 100–150 km altitude). Through the effects of gravity and pressure gradients, the plasma is then redistributed along the magnetic field line into the two bands of the EIA on either side of the equator.

[3] The EIA has been observed to often include four maxima with enhanced plasma densities in different longitudinal regions around the planet [e.g., *Sagawa et al.*, 2005; *Immel et al.*, 2006; *Kil et al.*, 2007; *Lin et al.*, 2007; *Jin et al.*, 2008; *Scherliess et al.*, 2008; *Wan et al.*, 2008]. This four-peaked structure has been attributed to the forcing by non-migrating tides originating in the lower atmosphere [e.g., *Immel et al.*, 2006; *Hagan et al.*, 2007; *England*, 2012]. Tides can modify the dynamo electric fields in the E-region and thereby extend their effects into the F-region ionosphere [e.g. *Heelis*, 2004]. As demonstrated by model studies, the DE3 tide (eastward propagating diurnal tide with zonal wave number 3) can produce the four-peaked longitudinal structure in the ionosphere [e.g. *Hagan et al.*, 2007; *Jin et al.*, 2008].

[4] Further, studies have found that the longitudinal structure of the EIA is subjected to periodic temporal modulations caused by atmospheric planetary waves [e.g. *Chen*, 1992; *Immel et al.*, 2009; *Liu et al.*, 2010a, 2010b]. These modulations correspond to the periods of planetary waves, and it is believed that these variations are produced through the interactions between the planetary waves and tides. It is generally believed that most planetary waves cannot propagate directly into the ionosphere [e.g. *Laštovička*, 2006]. However, by modulating tides their signatures could be carried into the E-region and subsequently into the ionosphere [*Laštovička*,

[1]Space Sciences Laboratory, University of California Berkeley, Berkeley, California, USA.
[2]Space Physics Laboratory, Vikram Sarabhai Space Center, Trivandrum, India.
[3]Haystack Observatory, Massachusetts Institute of Technology, Westford, Massachusetts, USA.

Corresponding author: G. Liu, Space Sciences Laboratory, University of California, Berkeley, CA 94720, USA. (guiping@ssl.berkeley.edu)

0148-0227/12/2012JA017588

2006; *Pancheva et al.*, 2006, 2008; *Pedatella and Forbes*, 2009]. Model studies have suggested that the planetary wave-tide interaction provides a means of communicating the planetary wave signature across a wide range of altitudes and latitudes [e.g. *Liu et al.*, 2010c; *Chang et al.*, 2010].

[5] Kelvin waves are one type of planetary wave that are generated in the troposphere by latent heat release [*Holton*, 1973; *Salby and Garcia*, 1987]. These waves are trapped in the equatorial region and propagate eastward with respect to the background flow. The Ultra Fast Kelvin (UFK) wave has a short period of 3–4 days and a vertical wavelength of 30–50 km [e.g. *Riggin et al.*, 1997; *Liberman and Riggin*, 1997; *Forbes*, 2000; *Takahashi et al.*, 2009]. Because of these properties, the wave can propagate upward into the mesosphere or even higher into the thermosphere, reaching significant amplitudes at these altitudes [e.g. *Forbes*, 2000; *Sridharan et al.*, 2002; *Pancheva et al.*, 2004; *Miyoshi and Fujiwara*, 2006; *Takahashi et al.*, 2005, 2007; *Forbes et al.*, 2009]. The UFK wave could directly modify the E- or F- region dynamo, thus potentially account for some of the day-to-day variability of the ionosphere. Indeed, studies have reported the presence of the 3-day variation in the equatorial region extending from the stratosphere into the ionosphere [*Takahashi et al.*, 2007]. Numerical simulations have shown Kelvin waves with realistic amplitudes (20–40 m/s) in the lower thermosphere can drive 25–50% perturbations in the total electron content [*Chang et al.*, 2010]. These provide evidence that the UFK wave can drive the day-to-day variation in the ionosphere.

[6] Recently, many studies have focused on studying the ionospheric changes associated with Sudden Stratospheric Warmings (SSWs) because SSWs are important for the global circulation of the atmosphere. Large perturbations have been observed for the F-region vertical plasma drifts during even a minor SSW [*Chau et al.*, 2009]. Enhanced lunar tide activity has also been found to occur simultaneously with SSWs [*Fejer et al.*, 2011]. *Chau et al.* [2012] present a review of the current understanding of the low-latitude response of the ionosphere to SSWs. Studying the consequences of SSWs on the ionospheric variability has become an intensively studied topic.

[7] The URSI World Day campaign in January 2010 coincides with a major SSW, and the campaign provides a coordinated set of observations of the ionospheric properties by the Incoherent Scatter Radar (ISR) at low latitude and midlatitude. These observations are of particular interest for studying the effects of SSWs on the ionosphere. They are also valuable for characterizing the ionosphere-atmosphere coupling in different latitudinal ranges.

[8] This study presents the UFK wave signature in the ionospheric variations at low latitudes and midlatitudes. The study uses the January 2010 URSI World Day campaign observations in combination with the global Total Electron Content (TEC) maps of the International GNNS Service (IGS) (GNNS: Global Navigation Satellite System) ground-based GPS product. A quasi-3-day (hereinafter referred to as 3-day) periodic variation is observed in the TEC maps at magnetic low latitudes during January 2010. Similarly, a 3-day UFK wave is observed at the same time in the neutral wind measurements at ~90 km altitude by a meteor radar at the magnetic equator. A detailed study of the identification of this wave is reported by *England et al.* [2012]. The month of January 2010 coincides with the onset of the SSW, but this wave occurs before the SSW and the 3-day wave often occurs in January [e.g., *Vincent*, 1993; *Yoshida et al.*, 1999; *Davis et al.*, 2011]. It is thus believed that this wave is not related to the SSW.

2. The 3-Day Periodic Variation in TEC

[9] IGS routinely provides a global GPS product, including the TEC maps at 2.5° × 5° latitude-longitude grids and 2 hour UT intervals with good spatial and temporal coverage. The TEC measurements made by the widely distributed network of ground-based GPS receivers are incorporated into the data product. Data gaps, such as those over the oceans where the GPS occultations are not available, are filled in through interpolations and data assimilation techniques [e.g. *Mannucci et al.*, 1998]. These products are finally validated against the TOPEX TEC data. The IGS TEC maps have been recognized and extensively used for studying the properties and variations of the ionosphere [e.g. *Wan et al.*, 2008; *Hernández-Pajares et al.*, 2009].

[10] The global IGS TEC maps are used in the present study to identify the day-to-day variations in the ionosphere. Because the UFK waves are trapped in the equatorial region, their effects on the ionosphere are expected to be seen at low latitudes near 15°–20°.

[11] Figure 1 presents the TEC maps on two successive days in January 2010 at 16 hour LT in the daytime hour. For this local time, sequences of the maps at various UT hours are selected and combined together. The figure shows that the distribution of TEC is asymmetric with respect to the magnetic equator, having the larger TEC value on the south side of the equator than on the north side. The largest TEC values are located at 10°–20°S magnetic latitude. This asymmetry, as expected for January, is a result of the offset of the magnetic equator, the subsolar point, and also the F-region meridional winds [*Thuillier et al.*, 2002].

[12] Figure 1 also shows the differences of the TEC maps from one day to another, suggesting a day-to-day change. They can be used to identify the periodic temporal variations on the periods of days. A continuous series of TEC maps from December 1, 2009 to Feb 28, 2010 are used to search for these variations during January 2010. The IGS TEC maps are interpolated at 1 hour UT intervals, and then they are selected for a given same local time. The data are also binned by magnetic latitude so the latitudinal variations are separated.

[13] Figure 2a gives the time series of the TEC values throughout January 1–31, 2010 at 20°S magnetic latitude. The TEC values are the largest in the southern hemisphere during the month of January, and so is the variation. This latitude is chosen and shown as an example. A wavelet transformation is applied to the series to determine its periodic signature. Figure 2b gives the corresponding wavelet spectrum, showing periods from 2 to 6 days. A strong 3-day signature is seen in the spectrum, and the variation occurs around days 15–27. This signature is statistically significant at the 95% confidence level.

[14] The 3-day signature is shown again in the periodogram of the global TEC data in Figure 3 for the selected days of January 15–27 when the 3-day signature is strongest. The magnetic latitudes extending from 40°S to 40°N are shown. The periodogram analysis is performed separately at

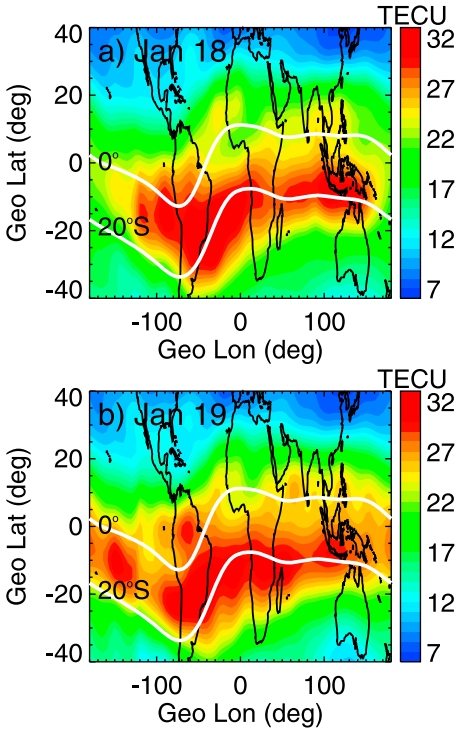

Figure 1. IGS TEC maps for the fixed LT of 16 hour for (a) January 18, 2010 and (b) January 19, 2010. The continents are outlined by the black lines on the plot. The overlapped white lines mark the magnetic equator and 20°S magnetic latitude. The TEC values presented are in TECU unit (1 TECU = 10^{16} electrons m^{-2}).

each latitude. The figure shows that the 3-day variation is observed between ±20° latitude. The variation is also observed at the higher latitude of 40°S but the amplitude is smaller. The signature is the strongest at 15°N and 15°S, but almost disappears at the magnetic equator. At the equator, a 2-day variation is observed but this signature is much weaker.

3. Internal and External Drivers of the 3-Day Variation

[15] The presence of the 3-day variation is observed in the day-to-day changes of TEC during January 2010. Drivers of this variation are investigated in this section. These include the internal forcing by atmospheric waves and the external drivers due to solar and geomagnetic activities. The mesospheric neutral wind observations are analyzed along with the f10.7 cm solar flux, the Kp index, and the International Reference Ionosphere (IRI) model output.

[16] The allSky Interferometer METeor (SKiYMET) radar at Thumba (8.5°N, 77°E), India has been regularly operated since 2004. This radar measures the neutral winds at 80–100 km altitude (at ~3 km bins) in the mesosphere and lower thermosphere. Throughout the month of January 2010, the radar was operated continuously and produced a time series of the hourly wind measurements. Thumba is located at the magnetic equator, so these data allow for the identification of the equatorial planetary waves, in particular the short period 3-day UFK wave. A detailed study of this wave in January 2010 has been presented by *England et al.* [2012].

[17] Figure 4 shows the 3-day component of the zonal wind measurement at 90 km altitude by the Thumba SKiYMET radar. The 3-day variation is the largest on days 16–23. This coincides with the occurrence of the 3-day variation of TEC (as shown in Figure 2). For a direct comparison, the 3-day

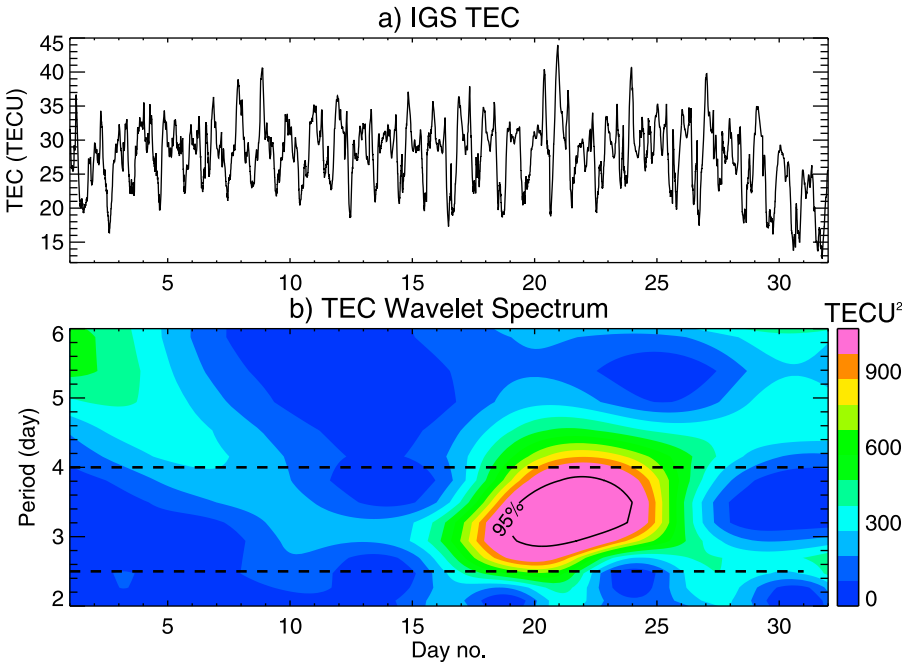

Figure 2. (a) Series of the IGS TEC values at 20°S magnetic latitude throughout January 1–31, 2010. (b) Wavelet spectrum of Figure 2a. The overlapped contour line gives the 95% confidence level of the wavelet spectrum. The dashed lines mark the 2.5-day and the 4-day period.

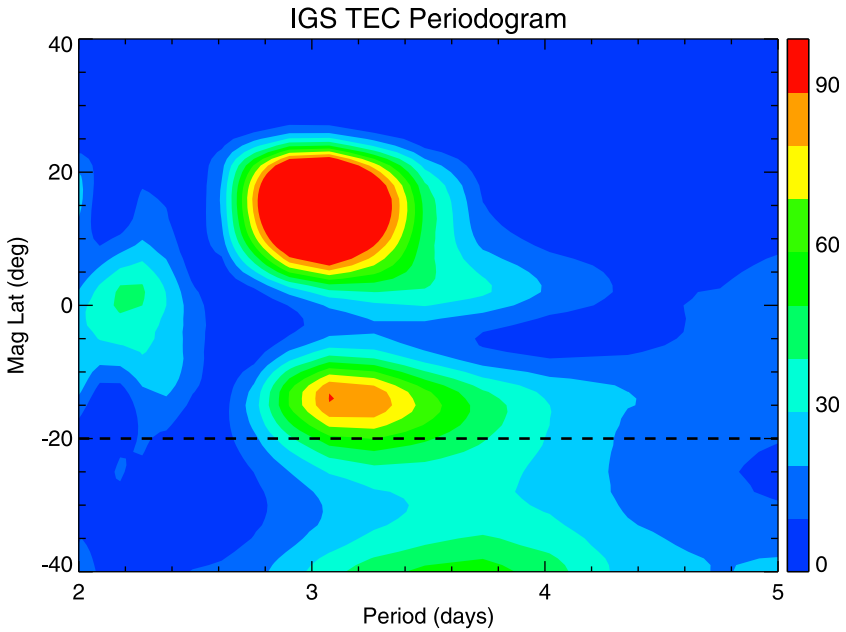

Figure 3. Lomb-scargle periodogram of the IGS TEC values for the selected time interval of January 15–27, 2010 at various magnetic latitudes. The dashed line marks the 20°S magnetic latitude that corresponds to Figures 2 and 4.

component of the TEC variation is shown together in Figure 4. The figure shows that the largest amplitude of the TEC variation occurs around days 17–24, being later than the 3-day wave in wind by about one day. This shows a close correspondence between the ionospheric variation and the 3-day wave in the atmosphere during January 2010. The TEC variation shown in the figure is for 20°S magnetic latitude, and it is most sensitive to the TEC values in the South American region (see Figure 1). The wind values are for Thumba, India (approximately 180° longitude away). Figure 4 shows that when the wind associated with the 3-day wave is westward/eastward over India/South America the TEC values over South America increase. The 3-day components of the ISR measurements are also included in the figure for electron densities measured at 330 km altitude over Millstone Hill (42.6°N, 71.5°W) and vertical ion velocities measured at 240 km altitude over Jicamarca (11.9°S, 76°W). The 3-day signature is present in the ISR measurements of these ionospheric properties at certain altitudes and its presence corresponds to the 3-day wave as well. The ionospheric response to this wave will be discussed in more detail in section 4.

[18] Figure 5 gives the daily f10.7 cm solar flux and the 3 hour Kp index on January 1–31, 2010. The solar flux is between 70 and 90 sfu and there is no sharp change of the value throughout this month. The Kp index is mostly at values of 0–2 except on January 20 the value is as great as 4. This value persists for only a few hours and quickly drops

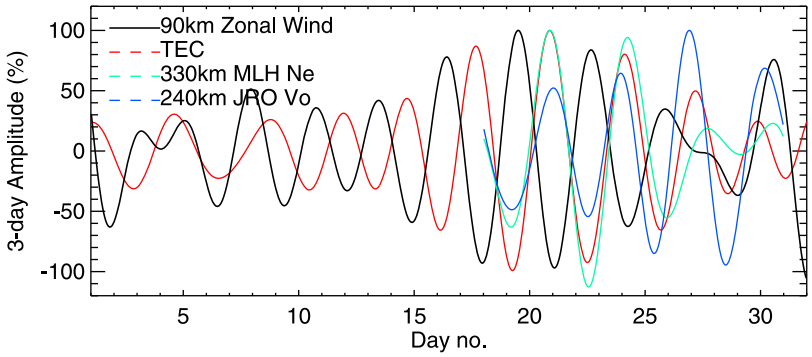

Figure 4. Normalized values of the 3-day component (normalized to the maximum value) in the zonal wind measurements by the Thumba SKiYMET radar at 90 km altitude (black line) and the IGS TEC (red line) at 20°S magnetic latitude throughout January 1–31, 2010. The 3-day components of the ISR measurements are included for electron density (N_e) at 330 km altitude over Millstone Hill (42.6°N, 71.5°W) (green line) and vertical ion velocity (V_o) at 240 km altitude over Jicamarca (11.9°S, 76°W) (blue line) during January 18–30, 2010.

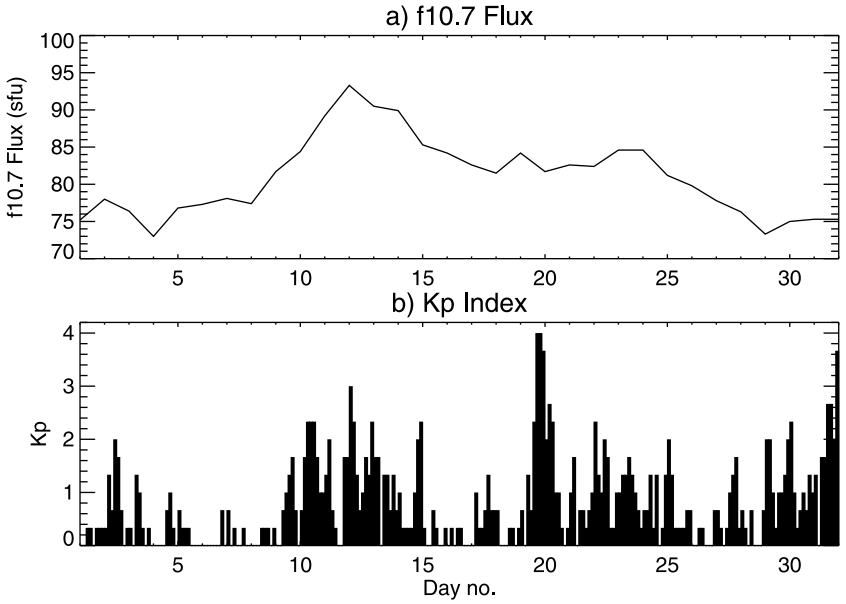

Figure 5. (a) Daily f10.7 cm radio fluxes for January 1–31, 2010. (b) The 3-hour Kp index for January 1–31, 2010.

to 2 the next day. The figure shows that the month of January 2010 is at the solar- and geomagnetically quiet conditions. Further, wavelet analysis of the solar wind speed observations and the solar irradiance observations (plots are not shown) does not show any coherent 3-day periodic variation that is correspondent to the TEC variation. The observed 3-day variation in TEC in January 2010 is mostly not driven by solar and magnetospheric drivers.

[19] The IRI model is a widely used standard for the specification of ionospheric parameters [e.g. *Bilitza*, 2001]. The IRI model can also be used to examine the possible drivers of the ionospheric variations. The output of the model are analyzed to establish whether any known external driver could produce the 3-day variation in TEC. Figure 6a shows the series of the modeled TEC values by IRI for 16 hour LT throughout January 1–31, 2010. These values are for the same LT and latitude as the IGS TEC observations presented in Figure 2. The IRI model predicts the large change of TEC associated with the diurnal cycle and the model also predicts a coherent increase of the value from January 20 to 31 which could be a seasonal change or possibly relates to Kp. However, the model result does not show any 3-day signature as

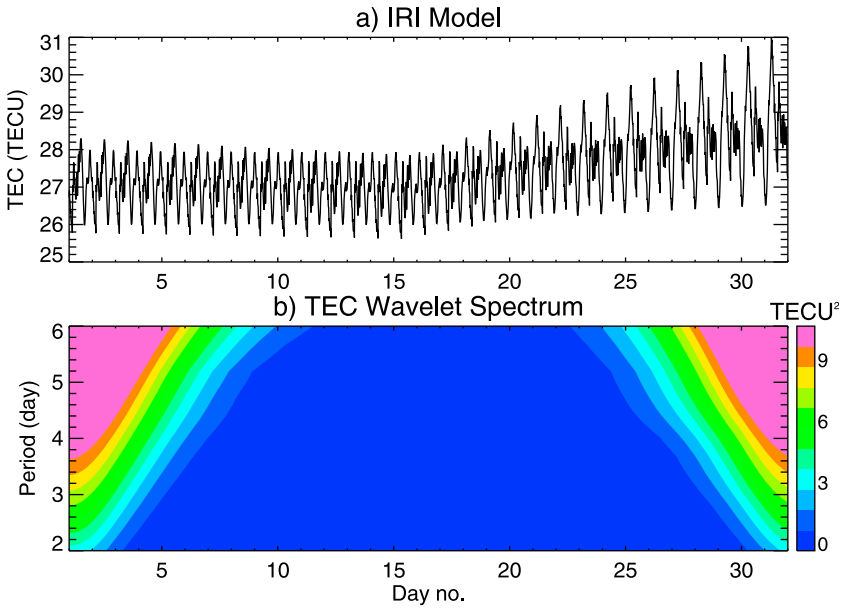

Figure 6. (a) Calculated TEC values by the IRI-2007 for 20°S magnetic latitude and 16 hour LT throughout January 1–31, 2010. (b) Wavelet spectrum of Figure 6a.

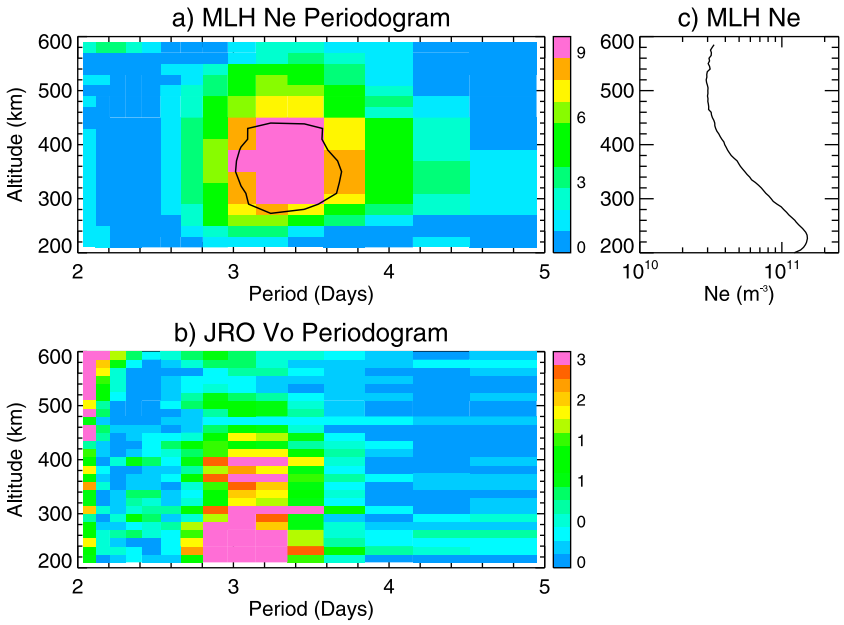

Figure 7. Lomb-scargle normalized periodogram of the ISR measurements for January 18–30, 2010 for (a) electron density N_e at Millstone Hill and (b) vertical ion velocity V_o at Jicamarca. The black curve overlapped denotes the 95% confidence level. (c) Averaged N_e profile observed by the Millstone Hill ISR at 16 hour LT throughout January 18–30, 2010. The profile shows that the peak of the F_2 layer is at ~220 km altitude.

seen in the observations in the IGS TEC. The forcing of the IRI model has not included any atmospheric wave. No credible solar or magnetic source produces the 3-day variation, while a 3-day wave is observed simultaneously in the atmosphere. The wave occurs at the same time as the 3-day TEC variation, and they have the similar latitudinal coverage. These show that the observed 3-day variation in TEC must be the result of the forcing by the 3-day wave.

4. Ionospheric Response to the 3-Day Wave as Seen by ISRs

[20] The URSI World Day campaign in January 2010 provided a coordinated set of observations of ISRs at different latitudes. During this campaign, the ISR at Jicamarca (11.9°S, 76°W) was operated continuously throughout January 18–February 4, and the Millstone Hill (42.6°N, 71.5°W) ISR was operated for January 18–30. The IGS TEC maps do not have the altitude information of the ionosphere because the GPS observations are height integrated quantities. On the contrary, the ISRs measure the ionosphere at different altitudes and their observations provide the altitude profiles of properties such as vertical ion drifts and electron densities. Here, these data are used to study the response of the ionosphere to the 3-day wave at low latitude and midlatitude.

[21] Figures 7a and 7b give the periodograms of the ISR observations in the altitude range of 200–600 km by Millston Hill for electron densities (N_e) and the Jicamarca radar for vertical ion drift velocities (V_o), respectively. Series of the radar observations at the same time interval of January 18–30 are used for the periodogram analysis for both radar sites. This time interval does not perfectly overlap with the 3-day variation of TEC (see Figure 2), but it includes all available ISR data. The figures present the strong 3-day signature in N_e between 300 and 500 km altitude over Millstone Hill (the signature is above the 95% confidence level). The signature is also seen in V_o throughout 200–400 km altitude at Jicamarca (it is not within the 95% confidence level which could be due to the large variance of V_o [e.g. *Alken*, 2009]). The 3-day signature is seen at different altitudes, and this provides a different measure of the confidence in the signature. Correspondingly, the amplitude of this 3-day variation is shown in Figures 8a and 8b for various altitudes. The occurrence of this variation in the ISR measurements has been shown in Figure 4. The presence of the 3-day signature is observed in these ionospheric observations by both radars at low latitudes and midlatitudes. As discussed in section 3, this signature is likely the result of the forcing by the atmospheric driver. The signature is observed at low latitudes and midlatitudes, showing a consistent response to the wave.

[22] The 3-day variation is observed at Millstone Hill at altitudes limited to 300–500 km (Figure 7a). The observations of TEC for the same location (the same latitude as Millstone Hill) do not include the 3-day variation (see Figure 3). To understand this difference, the altitude profiles of electron densities (N_e) observed by the Millstone Hill ISR are shown. Figure 7c gives the averaged profile at 16 hour LT throughout the operation interval of the radar during January 2010. The figure indicates that the peak height of the F_2 layer is at ~220 km altitude. The electron density drops quickly above the peak, having the value of only half of the peak density at the altitude of 300 km. The 3-day variation is seen at the altitudes much higher than the peak height. It is therefore reasonable the 3-day variation is not observed in the TEC data.

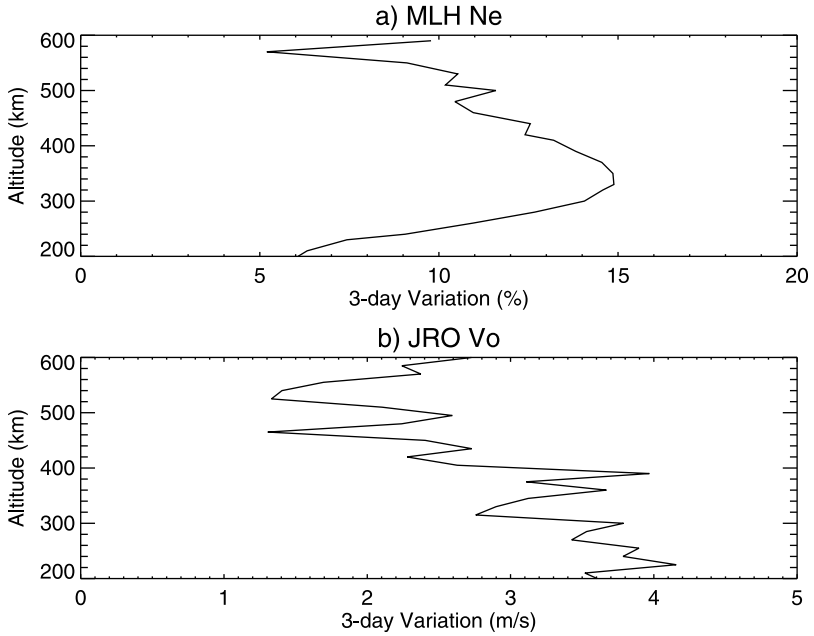

Figure 8. Amplitude of the 3-day variation observed during January 18–30, 2010 for (a) electron density N_e the Millstone Hill ISR and (b) vertical ion velocity drift the Jicamarca ISR. The 3-day variation of electron density is normalized to the mean value.

[23] The 3-day signature is not observed by the ISR at Millstone Hill in the vertical ion drift measurements (plot is not included). It is neither seen in the electron density observations at lower altitudes below the peak of the F_2 layer (shown in Figure 7a). In fact, the 3-day variation is only observed in the top side of ionosphere at this location. The 3-day wave is trapped within $\pm 30^\circ$ latitude [*England et al.*, 2012]. The 3-day signature observed at Millstone Hill could be from the lower latitude produced there by the 3-day wave through the electro dynamo action.

[24] Figure 9 illustrates conceptually how the 3-day wave signature is produced in the top side of ionosphere at Millstone Hill (as shown in Figure 7a). At lower latitudes, the 3-day wave modifies the E-region electric fields. The modulation of the electric field is immediately transmitted along the magnetic field line into the F-region. The resultant E × B drifts lift the plasma into higher altitude and higher latitude. Through the same process, the 3-day wave can also produce the signature as observed at Jicamarca (shown in Figure 7b). The E × B drifts produce the upward movement of the plasma at the magnetic

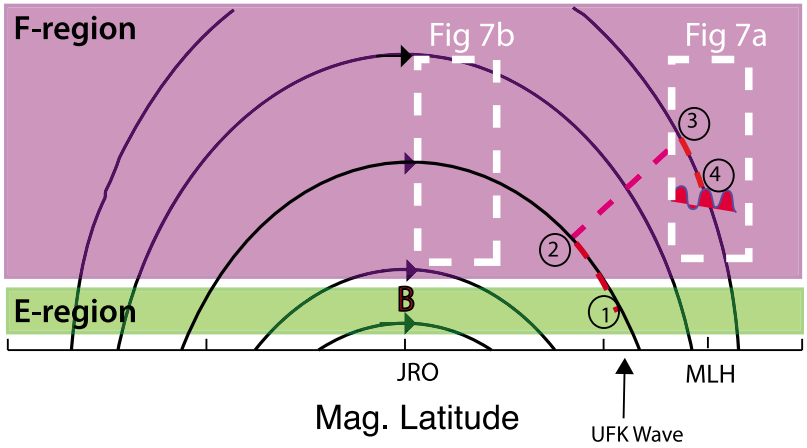

Figure 9. A cartoon describes how the 3-day wave signature is produced at Millstone Hill (marked as MLH on the plot). The process for producing this signature includes three steps. 1: The 3-day wave modifies the E-region electric fields at lower latitudes (the latitude limit the UFK wave can approach is marked), producing the 3-day modulation on the fields. 2: The modulation is transmitted into the F-region along the magnetic field line. 3: The resultant E × B drifts move the plasma into higher altitude and higher latitude, transmitting the 3-day signature into this region. 4: The plasma resides at midlatitude in the upper part of the F-region, showing the signature as seen in Figure 7a for Millstone Hill. The 3-day signature is also seen in the E × B drifts at Jicamarca (JRO) as shown in Figure 7b.

equator, so the 3-day signature is observed in the vertical ion drifts measurements. Following this, the plasma moves along the field line under the force of gravity and pressure gradients, and finally arrives at Millstone Hill in the top part of the F-region. As the vertical motion is at lower latitudes, the 3-day variation is not seen in the E × B drifts at Millstone Hill.

5. Discussion and Conclusions

[25] This study uses both atmosphere and ionosphere observations of multiple instruments as well as the model simulations by the IRI, focused on the case of January 2010. As this month coincides with a SSW, the URSI World Day campaign provides a coordinated set of observations of the ionosphere by ISRs at low latitudes and midlatitudes. The campaign data, in combination with the IGS global TEC maps and the neutral wind measurements by a meteor radar at the dip equator, are used to study the 3-day periodic variation observed in the ionosphere. External and internal drivers of the variations are investigated. The correspondence between the 3-day variation and the 3-day wave in the atmosphere is shown. The study finally reports the effects of the 3-day wave on the day-to-day variations of the ionosphere at low latitudes and midlatitudes as a function of altitude.

[26] The study finds a case of the electrodynamic coupling between the atmosphere and ionosphere during January 2010. During this month, the 3-day periodic variation is observed in the GPS TEC observations and the ISR observations at low latitudes and midlatitudes. The month is at solar- and geomagnetically quiet conditions, and the IRI model simulations do not indicate any 3-day signature due to external forcing. The observed ionospheric variation could be related to the 3-day wave in the atmosphere.

[27] The UFK 3-day wave originates in the lower atmosphere, and it can propagate upward into the mesosphere or the lower thermosphere [e.g *Forbes*, 2000; *Miyoshi and Fujiwara*, 2006; *Takahashi et al.*, 2007]. For January 2010, a 3-day wave is identified in the mesosphere. Detailed information on this wave has been given by *England et al.* [2012]. This 3-day wave can modify the E-region dynamo via either direct or indirect ways. Through these modulations, the wave signature can be transmitted into the E-region and subsequently into the F-region ionosphere.

[28] The study finds the 3-day wave signature in the top side of ionosphere at midlatitude. This signature is seen in the electron density observations at higher altitudes above the peak of the F_2 layer, but it is not seen in the vertical ion drift observations. These demonstrate that the 3-day wave signature is not produced locally. In fact, the signature could be from the lower latitude transmitted through modulations of the ionospheric dynamo at lower latitudes. This 3-day wave is trapped within $\pm 30^\circ$ latitude in the atmosphere [*England et al.*, 2012], but this study shows that the wave effects could reach the higher latitude as high as 40°N (50°N magnetic latitude).

[29] The UFK wave signature has been found in ionospheric properties such as the maximum frequency of the F_2 layer and the minimum virtual height [e.g. *Takahashi et al.*, 2007]. This study identifies the wave signature in the IGS GPS global TEC maps. These maps have an uniform and complete temporal and spatial coverage, so they are ideal for study the day-to-day variations and the planetary wave signatures in the ionosphere. The 3-day variation is also identified in the study in vertical drifts observations at Jicamarca and electron densities observations at Millstone Hill by the ISRs. These present the global impact of the 3-day wave on the ionospheric day-to-day variations at low latitudes and midlatitudes.

[30] **Acknowledgments.** This research work is supported by the National Science Foundation's CEDAR program through Award AGS-1042261 and NASA Heliophysics Research Program Award NNX12AD48G. Work at the MIT Haystack Observatory has been supported by NSF Cooperative Agreement ATM-0733510 with the Massachusetts Institute of Technology. The Jicamarca Radio Observatory is a facility of the Instituto Geofisico del Peru operated with support from the NSF AGS-0905448 through Cornell University. Data used in this study are available at http://wdc.kugi.kyoto-u.ac.jp for the f10.7 cm solar flux, ftp://ftp.ngdc.noaa.gov for the Kp index, http://omniweb.gsfc.nasa.gov for the IRI-2007 model, and http://cdaweb.gsfc.nasa.gov for the IGS GPS TEC product. The ISR data used are obtained from the Madrigal database at http://madrigal.haystack.mit.edu. The authors thank many personnel and institutes for making these data available.

[31] Robert Lysak thanks the reviewers for their assistance in evaluating the paper.

References

Alken, P. (2009), A quiet time empirical model of equatorial vertical plasma drift in the Peruvian sector based on 150 km echoes, *J. Geophys. Res.*, *114*, A02308, doi:10.1029/2008JA013751.

Appleton, E. (1946), Two anomalies in the ionosphere, *Nature*, *157*, 691.

Bilitza, D. (2001), International Reference Ionosphere 2000, *Radio Sci.*, *36*, 261–275.

Chang, L. C., S. E. Palo, H.-L. Liu, T.-W. Fang, and C. S. Lin (2010), Response of the thermosphere and ionosphere to an ultra fast Kelvin wave, *J. Geophys. Res.*, *115*, A00G04, doi:10.1029/2010JA015453.

Chau, J. L., B. G. Fejer, and L. P. Goncharenko (2009), Quiet variability of equatorial E × B drifts during a stratospheric warming event, *Geophys. Res. Lett.*, *36*, L05101, doi:10.1029/2008GL036785.

Chau, J. L., L. P. Goncharenko, B. G. Fejer, and H.-L. Liu (2012), Equatorial and low latitude ionospheric effects during sudden stratospheric warming events: Ionospheric effects during SSW periods, *Space Sci. Rev.*, doi:10.1007/s11214-011-9797-5, in press.

Chen, P.-R. (1992), Two-day oscillation of the equatorial ionization anomaly, *J. Geophys. Res.*, *97*, 6343–6357.

Davis, R. N., Y.-W. Chen, S. Miyahara, and N. J. Mitchell (2011), The climatology, propagation and excitation of ultra-fast Kelvin waves as observed by meteor radar, Aura MLS, TRMM and in the Kyushu-GCM, *Atmos. Chem. Phys. Diss.*, *11*, 29,479–29,525, doi:10.5194/acpd-11-29479-2011.

England, S. L. (2012), A review of the effects of non-migrating atmospheric tides on the Earth's low-latitude ionosphere, *Space Sci. Rev.*, doi:10.1007/s11214-011-9842-4, in press.

England, S. L., G. Liu, Q. Zhou, T. J. Immel, K. K. Kumar, and G. Ramkumar (2012), On the signature of the quasi-3-day wave in the thermosphere during the January 2010 URSI World Day Campaign, *J. Geophys. Res.*, doi:10.1029/2012JA017558, in press.

Fejer, B. G., B. D. Tracy, M. E. Olson, and J. L. Chau (2011), Enhanced lunar semidiurnal equatorial vertical plasma drifts during sudden stratospheric warmings, *Geophys. Res. Lett.*, *38*, L21104, doi:10.1029/2011GL049788.

Forbes, J. M. (2000), Wave coupling between the lower and upper atmosphere: case study of an ultra-fast Kelvin Wave, *J. Atmos. Sol.-Terr. Phys.*, *62*, 1603–1621.

Forbes, J. M., Zhang, X. L., Palo, S. E., Russell, J., Mertens, C. J., and Mlynczak, M. (2009), Kelvin waves in stratosphere, mesosphere and lower thermosphere temperatures as observed by TIMED/SABER during 2002–2006, *Earth Planets Space*, *61*, 447–453.

Hagan, M. E., A. Maute, R. G. Roble, A. D. Richmond, T. J. Immel, and S. L. England (2007), Connections between deep tropical clouds and the Earth's ionosphere, *Geophys. Res. Lett.*, *34*, L20109, doi:10.1029/2007GL030142.

Heelis, R. A. (2004), Electrodynamics in the low and middle latitude ionosphere: a tutorial, *J. Atmos. Sol.-Terr. Phys.*, *66*, 825–838.

Hernández-Pajares, M., J. M. Juan, J. Sanz, R. Orus, A. Garcia-Rigo, J. Feltens, A. Komjathy, S. C. Schaer, and A. Krankowski (2009), The IGS VTEC maps: A reliable source of ionospheric information since 1998, *J. Geod.*, *83*, 263–275, doi:10.1007/s00190-008-0266-1.

Holton, J. R. (1973), On the frequency distribution of atmospheric Kelvin waves, *J. Atmos. Sci.*, *30*, 499-500.

Immel, T. J., E. Sagawa, S. L. England, S. B. Henderson, M. E. Hagan, S. B. Mende, H. U. Frey, C. M. Swenson, and L. J. Paxton (2006), Control of

equatorial ionospheric morphology by atmospheric tides, *Geophys. Res. Lett. 33*, L15108, doi:10.1029/2006GL026161.
Immel, T. J., S. L. England, X. Zhang, J. M. Forbes, and R. DeMajistre (2009), Upward propagating tidal effects across the E- and F-regions of the ionosphere, *Earth Planets Space*, *61*, 1–11.
Jin, H., Y. Miyoshi, H. Fujiwara, and H. Shinagawa (2008), Electrodynamics of the formation of ionospheric wave number 4 longitudinal structure, *J. Geophys. Res.*, *113*, A09307, doi:10.1029/2008JA013301.
Kil, H., S.-J. Oh, M. C. Kelley, L. J. Paxton, S. L. England, E. Talaat, K.-W. Min, and S.-Y. Su (2007), Longitudinal structure of the vertical E × B drift and ion density seen from ROCSAT-1, *Geophys. Res. Lett.*, *34*, L14110, doi:10.1029/2007GL030018.
Laštovička, J. (2006), Forcing of the ionosphere by waves from below, *J. Atmos. Sol. Terr. Phys.*, *68*, 479–497.
Liberman, R. S., and D. Riggin (1997), High resolution doppler imager obervations of Kelvin waves in the equatorial mesosphere and lower thermosphere, *J. Geophys. Res.*, *102*, 26,117–26,130, doi:10.1029/96JD02902.
Lin, C. H., W. Wang, M. E. Hagan, C. C. Hsiao, T. J. Immel, M. L. Hsu, J. Y. Liu, L. J. Paxton, T. W. Fang, and C. H. Liu (2007), Plausible effect of atmospheric tides on the equatorial ionosphere observed by the FORMOSAT3/COSMIC: Three-dimensional electron denstity structure, *Geophys. Res. Lett. 34*, L11112, doi:10.1029/2007GL029265.
Liu, G., T. J. Immel, S. L. England, K. K. Kumar, and G. Ramkumar (2010a), Temporal modulations of the longitudinal structure in F_2 peak height in the equatorial ionosphere as observed by COSMIC, *J. Geophys. Res.*, *115*, A04303, doi:10.1029/2009JA014829.
Liu, G., T. J. Immel, S. L. England, K. K. Kumar, and G. Ramkumar (2010b), Temporal modulations of the four-peaked longitudinal structure of the equatorial ionosphere by the 2 day planetary wave, *J. Geophys. Res.*, *115*, A12338, doi:10.1029/2010JA016071.
Liu, H.-L., W. Wang, A. D. Richmond, and R. G. Roble (2010c), Ionospheric variability due to planetary waves and tides for solar minimum conditions, *J. Geophys. Res.*, *115*, A00G01, doi:10.1029/2009JA015188.
Mannucci, A. J., B. D. Wilson, D. N. Yuan, C. M. Ho, U. J. Lindqwister, and T. F. Runge (1998), A global mapping technique for GPS-derived ionospheric total electron content measurements, *Radio Sci.*, *33*, 565–582.
Miyoshi, Y., and H. Fujiwara (2006), Excitation mechanism of intraseason oscillation in the equatorial meososphere and lower thermosphere, *J. Geophys. Res.*, *111*, D14108, doi:10.1029/2005JD006993.
Namba, S., and K. I. Maeda (1939), Radio wave propagation, Corona, Tokyo.
Pancheva, D. V., N. J. Mitchell, and P. T. Younger (2004), Meteor radar observations of atmospheric waves in the equatorial mesosphere/lower thermosphere over Ascension Island, *Ann. Geophys.*, *22*, 387–404, doi:10.5194/angeo-22-387-2004.
Pancheva, D. V., et al. (2006), Two-day wave coupling of the low-latitude atmosphere-ionosphere system, *J. Geophys. Res.*, *111*, A07313, doi:10.1029/2005JA011562.
Pancheva, D. V., et al. (2008), Planetary wave coupling (5–6 day waves) in the low-latitude atmosphere-ionosphere system, *J. Atmos. Sol. Terr. Phys.*, *70*, 101–122.
Pedatella, N. M., and J. M. Forbes (2009), Modulation of the equatorial F-region by the quasi-16-day planetary wave, *Geophys. Res. Lett.*, *36*, L09105, doi:10.1029/2009GL037809.
Riggin, D. M., D. C. Fritts, T. Tsuda, T. Nakamura, and R. A. Vincent (1997), Radar observations of a 3-day Kelvin wave in the equatorial mesosphere, *J. Geophys. Res.*, *102*, 26,141–26,158, doi:10.1029/96JD04011.
Sagawa, E., T. J. Immel, H. U. Frey, and S. B. Mende (2005), Longitudinal structure of the equatorial anomaly in the nighttime ionosphere observed by IMAGE/FUV, *J. Geophys. Res.*, *110*, A11302, doi:10.1029/2004JA010848.
Salby, M. L., and R. R. Garcia (1987), Transient response to localized episodic heating in the tropics. Part I: Excitation and short-time near field behavior, *J. Atmos. Sci.*, *44*, 458–498.
Scherliess, L., D. C. Thompson, and R. W. Schunk (2008), Longitudinal variability of low-latitude total electron content: Tidal influences, *J. Geophys. Res.*, *113*, A01311, doi:10.1029/2007JA012480.
Sridharan, S., S. Gurubargan, and R. Rajaram (2002), Radar observations of the 3.5-day ultra-fast Kelvin wave in the low-latitude mesopause region, *J. Atmos. Sol-Terr. Phys.*, *64*, 1241–1250, doi:10.1016/S1364-6826.
Takahashi, H., L. M. Lima, C. M. Wrasse, M. A. Abdu, I. S. Batista, D. Gobbi, R. A. Buriti, and P. P. Batista (2005), Evidence on 2–4 day oscillation of the equatorial ionosphere h′F and mesosphere airglow emissions, *Geophys. Res. Lett.*, *32*, L12102, doi:10.1029/2004GL022318.
Takahashi, H., et al. (2007), Signatures of ultra fast Kelvin waves in the equatorial middle atamosphere and ionosphere, *Geophys. Res. Lett.*, *34*, L11108, doi:10.1029/2007GL029612.
Takahashi, H., et al. (2009), Possible influence of ultra-fast Kelvin wave on the equatorial ionosphere evening uplifting, *Earth Planets Space*, *61*, 455–462.
Thuillier, G., R. H. Wiens, G. G. Shepherd, and R. G. Roble (2002), Photochemistry and dynamics in thermospheric intertropical arcs measured by the WIND Imaging Interferometer on board UARS: A comparison with TIE-GCM simulations, *J. Atmos. Sol. Terr. Phys.*, *64*, 405–415.
Vincent, R. (1993), Long-period motions in the equatorial mesosphere, *J. Atmos. Terr. Phys.*, *55*(7), 1067–1080, doi:10.1016/0021-9169(93)90098-J.
Wan, W., L. Liu, X. Pi, M.-L. Zhang, B. Ning, J. Xiong, and F. Ding (2008), Wavenumber-4 patterns of the total electron content over the low latitude ionosphere, *Geophys. Res. Lett.*, *36*, L12104, doi:10.1029/2008GL033755.
Yoshida, S., T. Tsuda, A. Shimizu, and T. Nakamura (1999), Seasonal variations of 3.0–3.8 day Ultra-fast Kelvin waves observed with a meteor wind radar and radiosonde in Indonesia, *Earth Plan. Space*, *51*, 675–684.